Instrumental Development

(BL8A)

Carbon contamination of SR mirror

Eiken Nakamura[1], Mikito Tadano[2], Hiroshi Sakai[2], Nobuhiro Terumuma[2], Masami Hasumoto[1], Junji Urakawa[2], Takashi Naito[2], Yasunori Tanimoto[2], Eiji Shigemasea[1]

[1] *Institute for Molecular Science, Okazaki 444-8585, Japan*

[2] *High Energy Accelerator Research Organization , 1-1 Oho Tsukuba 305-0801,Japan*

When SR irradiates an optical device, it is known well that carbon contamination will arise in an irradiation part. Carbon pollution of the optical device is a serious problem for the measurement of a SR beam line. Some kinds of optical measurement in carbon region have been made under the very difficult situation according to the experience of UVSOR. At KEK-ATF, the beam size measurement experiment in a visible region has been affected. It is coped with by exchanging the optical element polluted until now. It is important to remove or mitigate carbon contamination for the measurement of SR beam lines. We aim at finding the environment in which carbon contamination does not generate.

In order to investigate the growth rate of carbon contamination, the experiment has been performed by BL8A. The growth rate was compared by the measurement of the reflective intensity of laser light of 670nm with different conditions. The reflective intensity from SR irradiation part and a non-irradiation part was simultaneously measured, and the surface temperature and surface current of a mirror were also measured. We used three kinds of mirrors (Au coat mirror, Al coat mirror and Pt coat mirror). The experiment of this time was to measure the difference of reflection materials, gas purge effect and magnetic field effect.

Fig.1 shows the reflectivity as function of dose in three kinds of reflection materials of Au, Al and Pt. The material's dependence of the carbon contamination was clearly measured. However, an inspection of mirrors after SR irradiation indicates the contamination on both Al coat mirror and Au coat mirror, and not it on Pt coat mirror.

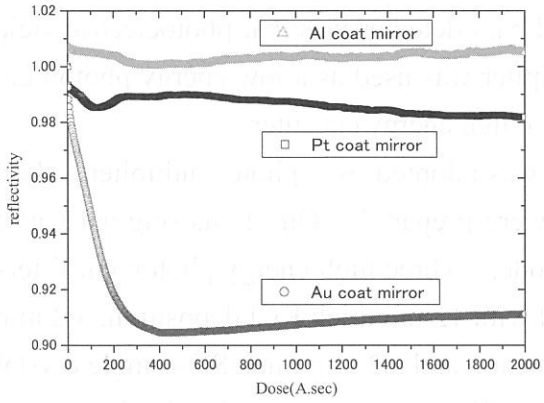

Fig.1: Reflectivity as a function of dose for reflection materials.

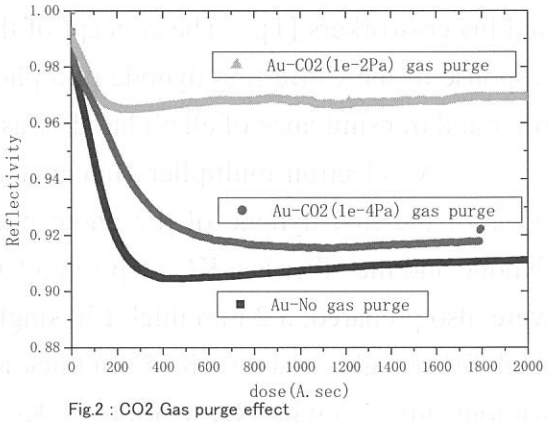

Fig.2 : CO2 Gas purge effect

The effect of a CO2 gas purge was investigated about an Au coat mirror (Fig.2). The reflection rate changes according to CO2 gas pressure. It is not clear whether the change comes from ozone generation by CO2-photon reaction or photon decrease by the absorption. The magnetic field effect was measured on Au coat mirror. There was no remarkable change in reflectance. However, the surface current was changing according to magnetic field intensity (Fig.3).

We have also measured about other effects. Interesting results were provided and can be expected in future experiment.

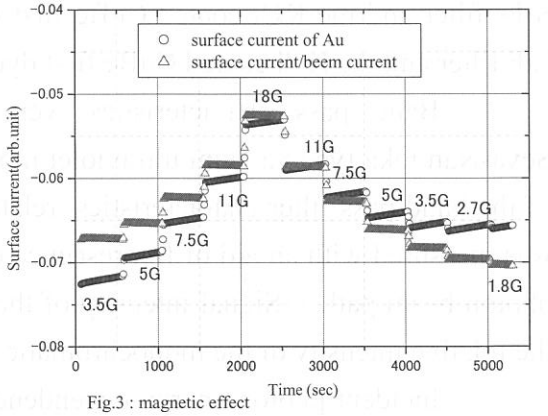

Fig.3 : magnetic effect

Referrence

[1] T.Naito et.al., *UVSOR Activity Report*, 2000, P63

(BL1B)

Characteristics of Vacuum Ultraviolet Region Band Pass Photon Detector for Inverse Photoelectron Spectrometer

Shojun Hino, Hiroyuki Kagitani and Kentaro Iwasaki

Faculty of Engineering and Graduate School of Science and Technology,
Chiba University, Inage-ku, Chiba Japan 263-8522

Inverse photoelectron spectroscopy is a powerful tool to investigate unoccupied electronic states. Inverse photoelectron spectrometer can be classified mainly into two categories according to the way of the measurement of emitted photon; one is using a monochromator of vacuum ultraviolet region and the other is using a photon band pass filter. We are now constructing an inverse photoelectron spectrometer equipped with the band pass filter constituted with an photo multiplier and an alkali halide window material, since band pass filters are less expensive and easily assembled to the vacuum chamber. In this report we describe the characteristics of our band pass photon detector of vacuum ultraviolet region.

Band pass detectors were fabricated according to the design proposed by Yokoyama and his co-workers [1]. The concept of their band pass detector was that photoelectric yield response of the CuBe first dynode of a photo multiplier was used as a low energy photon cut filter and transmittance of alkali halide was used as a high energy cut filter.

An electron multiplier Hamamatsu R595 was adopted as a photo multiplier. Two types of the first dynode of the photo multiplier were prepared. One is its original CuBe dynode and the other is a KCl deposited CuBe dynode. Three high energy photon cut filters were also prepared; a 2 mm thick LiF single crystal with 15 nm thick KCl deposition, a 2 mm thick SrF_2 single crystal with 15 nm thick KCl deposition and a 2 mm thick SrF_2 single crystal without any coating. Deposition of KCl onto the filters served to make the band pass narrower. We examined three types band pass detectors; detector A consists of the KCl coated SrF_2 filter and the normal CuBe first dynode, detector B consists of the KCl coated SrF_2 filter and the KCl coated CuBe first dynode and detector C consists of the KCl coated LiF filter and the KCl coated CuBe first dynode.

Band pass characteristics were measured at BL1B of UVSOR (a 1 meter Seya-Namioka type vacuum ultraviolet monochromator). Before and after the measurement of the band pass filter characteristics, relative photon intensity of the monochromatized light was measured with an aid of fluorescence emitted from a sodium salicylate film placed at the photon beam path. Signal intensity of the band pass detectors was normalized according to the relative intensity of the monochromatic light.

Incident photon energy dependence of three band pass detectors is shown in Fig. 1. Detector A has maximum sensitivity at 9.47 eV with 0.7 eV full width at half maximum

(FWHM) and its sensitivity is pretty low. Detector B shows maximum sensitivity at 9.5 eV with 0.5 eV FWHM. Deposition of KCl onto the first dynode (detector B) improves the sensitivity of the photon detector about three time compared with no KCl coated one (detector A) and pass energy width by 0.2 eV. It seems that detector B can be used as a narrow and sensitive band pass photon detector. The behavior of detector C is quite different from that of detectors A and B. Detector C has maximum sensitivity at 11.48 eV and with much wider FWHM of 1.85 eV. Its sensitivity is about ten times better than that of detector B, which is advantageous for the inverse photoelectron measurement of organic materials that is easily damaged by irradiation of electron beam. However, its wide FWHM together with a shoulder structure at 10.5 eV could be a serious problem for the materials that have unoccupied states situated very closely each other. Thus the best choice for the photon detector in the inverse photoelectron measurement may be detector B for less electron beam sensitive materials with crowded unoccupied states and detector C for electron beam sensitive materials with widely spaced unoccupied states.

References

[1] K. Yokoyama, K. Nishihara, K. Mimura, Y. Hari, M. Taniguchi, Y. Ueda, and M. Fujisawa, Rev. Sci. Instrum. 64, 87 (1993).

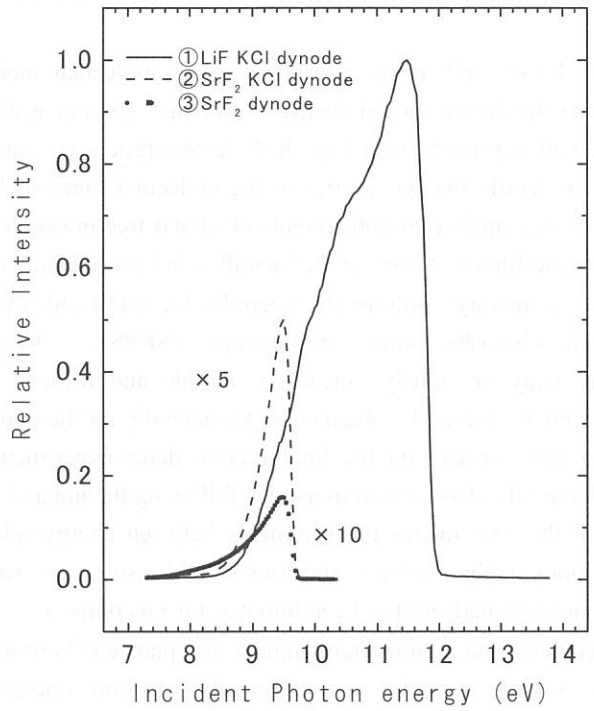

Fig. 1 Spectral response of three band pass photon detectors.

(BL4B)

New Apparatuses for Coincidence Measurements towards Understanding Dissociation Dynamics of Inner-Shell Excited Molecules

E. Shigemasa, N. Kondo, E. Nakamura, and T. Gejo

Institute for Molecular Science, Okazaki 444-8585, JAPAN

Thanks to the rapid progress of experimental techniques related to synchrotron radiation, vibrational spectroscopy in the inner-shell excitation region of low-Z molecules becomes feasible. The findings in the recent observations of the resonant Auger processes and their theoretical analyses impel us to give up the traditional idea that the molecular dissociation starts at the Auger final state where the Auger transition is terminated. This means that the Auger decay can not be treated separately from the primary photoexcitation process, that is, "break down of the two step model". In the case of photoionizaiton processes, the so-called post collision interaction (PCI) effect, which occurs in the Auger decay followed by near-threshold inner-shell photoionization due to the interaction between the Auger electron and the corresponding photoelectron, is known to illustrate such a situation. In addition, the contribution of multiple excitations owing to the electron correlation makes molecular inner-shell excitation processes near the thresholds complicated. Threshold electron spectroscopy (TES) is one of the most powerful techniques for probing the multiple excitations. A novel threshold electron spectrometer has been constructed for this purpose. The spectrometer is composed of a lens system based on the penetrating field technique [1] and an electrostatic analyzer (Comstock inc. AC-901 model), and its performance test is just beginning to be carried out. It is seen from the trajectories for photoelectrons with 5 meV kinetic energy shown in Fig. 1 that the potential well collects the threshold electrons over all angles. The asymmetric trajectories observed in Fig. 1 are due to the influence of the potential on the gas nozzle.

The interpretation of the spectral features observed in the molecular inner-shell excitation spectra is essential towards understanding the dissociation dynamics, since the subsequent decay processes never happen without the primary photoexcitation process even though these two processes can not be treated separately as mentioned above. In order to identify the symmetries of the molecular inner-shell excited states, polarization dependent studies have been widely applied to both chemisorbed and free molecules. For diatomic molecules, the measurements of the energetic fragment ions emitted parallel and perpendicular to the electric vector of the incident light achieve complete symmetry resolution between the $\Delta\Lambda=0$ (Σ) and $\Delta\Lambda=1$ (Π) transitions [2], which is called symmetry-resolved photoabsorption spectroscopy (SRPS). Recent high-resolution SRPS measurements for N_2 reveal many previously unresolved double and triple excitations. Further detailed information on the multiple excitations may be obtained experimentally by the combination of SRPS and TES. The construction of a new apparatus for realizing this kind of coincidence experiments has begun.

For detailed investigation on the dissociation dynamics following the inner-shell excitation and ionization, it is indispensable to perform the coincidence measurements between energy-selected electrons and ions, in which the angular distributions of the electrons and ions should also be measured. The construction of a high luminosity electrostatic electron analyzer has been initiated for this purpose. The design of the analyzer is based on a double toroidal geometry and an important angular acceptance (5% of 4π) [3]. Its two-dimensional position sensitive detection system provides simultaneously electron energy and angular distribution measurements. Fig. 2 shows a three dimensional view of the mechanical setup of the double toroidal analyzer. The test operation will be started in the near future.

References

[1] R.I. Hall et al., *Meas. Sci. Tech.* **3**, 316 (1992).

[2] E. Shigemasa et al., *Phys. Rev. A* **45**, 2915 (1992).
[3] C. Miron et al., Rev. Sci. Instrum. **68**, 3728 (1997).

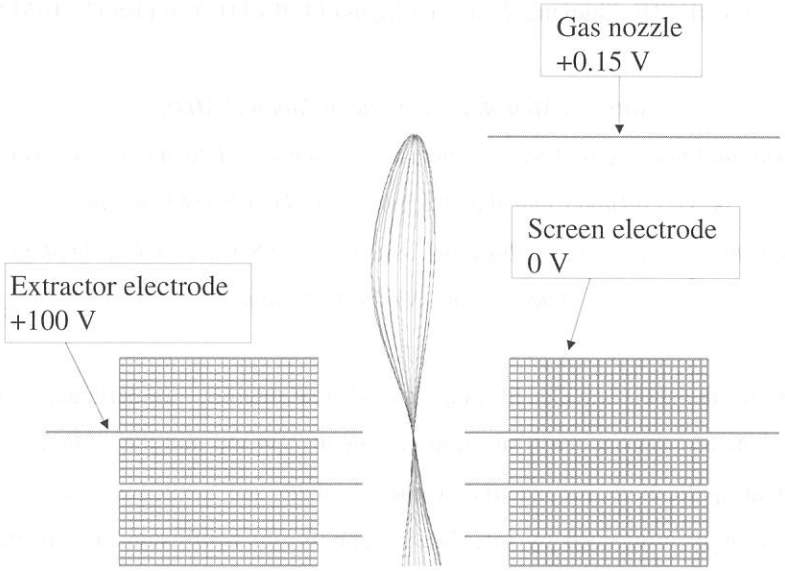

Fig. 1. Electron trajectories in the penetrating field geometry.

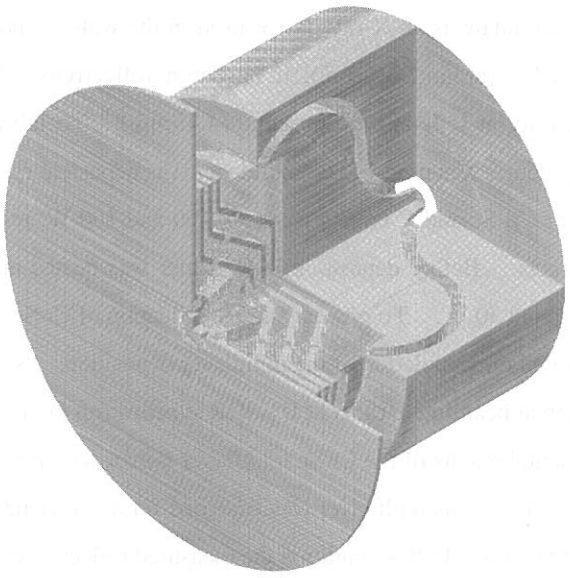

Fig. 2. Three dimensional view of the double toroidal analyzer.

(BL5B)

Reflectivity Measurements of Cr/Sc and Cr/C Multilayers for Soft X-rays

Tadayuki OHCHI, Shiqiang WEI*, Toshiyuki FUJIMOTO and Isao KOJIMA

National Metrology Institute of Japan (NMIJ),
National Institute of Advanced Industrial Science and Technology (AIST)
AIST Tsukuba Central 5, Tsukuba, Ibaraki 305-8565, Japan
**National Synchrotron Radiation Laboratory, University of Science and Technology of China*
Hefei, Anhui 230029, P.R.China

X-ray multilayers for the short wavelength range are of great interest. In particularly, multilayers for the water window region between the oxygen K-absorption edge at 2.34 nm and the carbon K-absorption edge at 4.38 nm have important applications for material science, biology and medicine. The reflectivity of such a multilayer mirror is strongly influenced by interface roughness, inter-diffusion and fluctuation of the layer thickness, because the layer thickness is extremely small. Thus fabricating multilayer with high performance is very difficult in this region. In order to fabricate the high performance X-ray multilayer mirror, it is necessary to prepare the multilayer films with high precisely and to analyze their structural properties for the improvement of its performance.

Cr/Sc multilayer mirror is a candidate as an X-ray mirror used in the water window region. Especially at just above the Sc L-absorption edge (around 3.11nm), it has high reflectivity. On the other hand, Cr/C multilayer mirror has high reflectivity at C K-absorption edge (4.48 nm). To fabricate these mirrors the r.f. magnetron sputtering deposition system [1] was used. The multilayer was deposited on SiO_2 wafer under an argon gas atmosphere. The rf powers of Cr, Sc and C targets were 50, 100 and 100 W, respectively. The argon gas flow rate was 2.5 sccm for all targets. Before deposition, SiO_2 wafer was heated at 200 °C in 30 minutes for cleaning and then cooled down to about 30 °C. To prevent surface oxidation of Cr/Sc multilayer, a carbon film of about 2 nm in thickness was deposited on completion of the multilayer deposition. Soft X-ray reflectivities were measured with s-polarized radiation at beamline BL-5B at UVSOR synchrotron facility.

Figure 1 and 2 show experimental results of the Cr/Sc multilayer mirror with periodic thickness of about 3.4 nm and 50 layer pairs (Multilayer #1). This multilayer was designed for a wavelength of 3.37 nm (C VI 1s-2p emission) and an incident angle of 60 deg. In this condition the measured reflectivity was about 8.74 % shown in Fig. 1. This was about 40 % of the reflectivity with an ideal interface. The main reason of reduction of reflectivity is roughness. In this case, roughnesses on the top interface of Cr and Sc layers were about 0.5 and 0.6 nm, respectively. The maximum reflectivity around Sc L-absorption edge shown in Fig. 2 was about 20.4 % at the wavelength of 3.16 nm and the incident angle of 62.5 °.

Figure 3 shows the result of the Cr/Sc multilayer mirror with periodic thickness of about 1.95 nm and 80 layer pairs (Multilayer #2). This multilayer was designed for an incident angle of 30 deg. In this condition the measured reflectivity was about 1.3 %. The reflectivity around Sc L-absorption edge 2 was about 4.3 % at the wavelength of 3.12 nm and the incident angle of 36.6 °.

The reflectivity of the Cr/C multilayer mirror with periodic thickness of about 5.18 nm and 8 layer pairs (Multilayer #3) was measured. This multilayer was designed for a wavelength of 4.47 nm (C Kα line) and an incident angle of 60 deg. The reflectivity was about 0.5 % at an incident angle of 55 deg. It was very low and an incident angle was different from designed one. This was because thickness of carbon layer was fluctuated caused by unstable carbon plasma.

References

1) T. Fujimoto, B. Li, I. Kojima, S. Yokoyama, and S. Murakami, *Rev. Sci. Instr.*, 70, 4362 (1999).

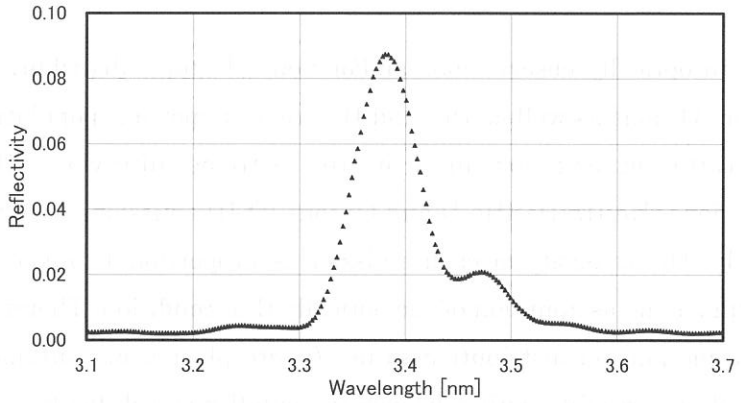

Fig. 1 Reflectivities of Multilayer #1 at an incident angles of 60.0 deg.

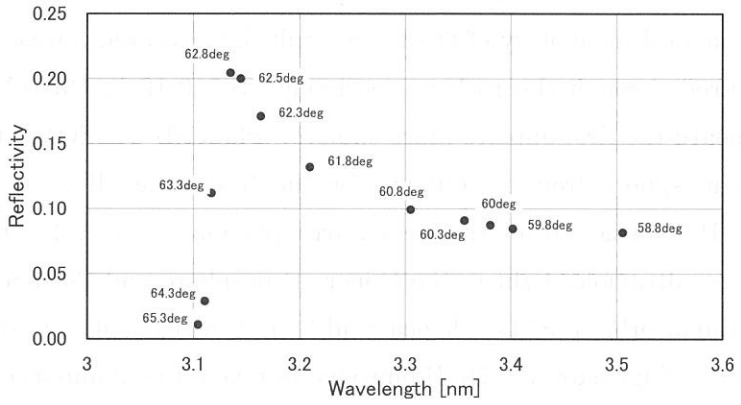

Fig. 2 Peak reflectivities of Multilayer #1 at each incident angle.

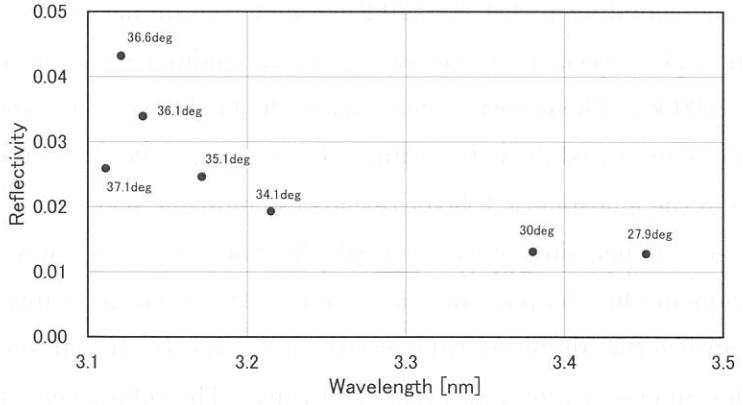

Fig. 3 Peak reflectivities of Multilayer #2 at each incident angle.

(BL5B)

Optical Characteristics of Mo/Si Multi-layer Evaporated using the Magnetron DC/RF Sputtering System

[A]M. Nakamura, [A]T. Murachi, [B]I. Yoshikawa, [A]Y. Takei, and [C]A. Yamazaki

[A] *Department of Earth and Planetary Science, University of Tokyo, Bunkyo-ku 113-0033*

[B] *Institute of Space and Astronautical Science, Sagamihara, Kanagawa 229-8510*

[C] *Communications Research Laboratory, Koganei, Tokyo 184-8795*

We study to optically observe ions and/or neutral atoms distribution in space plasma environments, where O^+ ions as well as He^+ and He are an important population. These particles have resonance scattering emission lines in the extreme ultraviolet (EUV) region. The wavelengths of He^+ ions (He II), He (He I) and O^+ ions (O II) emissions are 30.4nm, 58.4nm and 83.4nm, respectively. The intensity of each emission is proportional to column density of each scattered particle under the assumption of the optically thin condition. Therefore a 2-D snap shot brings the macroscopic plasma distribution to us. *In-situ* plasma measurements limited to the very close vicinity of one satellite with a low-energy cutoff has a difficulty in identifying global distribution and transport mechanisms of the cold plasmas.

The fundamental technology of the Mo/Si multi-layer coated mirror for detecting He II emission was acquired through the rocket experiments S-510-19 [1]. Our eXtreme Ultra-Violet (XUV) Scanner onboard the first Japan's Mars explorer, Planet-B (NOZOMI) took the imaging of the terrestrial plasmasphere from its outside for the first time all over the world [2), 3)] and discovered the He II emission from the near-Earth plasma sheet [4]. In the near future the Telescope of EXtreme ultraviolet light in the Upper- atmosphere and Plasma Imager component (UPI-TEX) for the Lunar orbiter, SELenological and ENgineering Explorer (SELENE), which will be launched in 2005, will measure the He II emission to reveal the abundance and distribution of He^+ ions in the terrestrial plasmasphere. Furthermore we developed the extreme ultraviolet (XUV) sensor for the sounding rocket SS-520-2 without contamination from the very strong H Lyman-α emission, and succeed in the observing the altitudinal variation of the O II emission from 150 through 1100 km. The observed intensity of the O II emission beyond an expectation at the topside ionosphere indicated the extraordinary O^+ ions lying over the ionosphere. And also the high emission rate in the ionospheric F layer reveals the multiple scattering effects.

For the next generation of the optical observation we are developing the imaging spectroscopy instruments for the planetary atmosphere and ionosphere imaging in a broadband EUV range. We improve the Mo/Si multi-layer coating for the He II emission described above to apply the mirror for an observation in a broadband range. The reflectively of a Mo/Si coated test piece mirror, which was evaporated using the magnetron DC/RF sputtering system at the Communications Research Laboratory (CRL), was measured to estimate the optical constant.

Figure shows the measured reflectively of the test piece at 30.4-nm wavelength (point) and calculated values for the Mo 5nm/Si 33nm multi-layer coating (curve). Since two wave structures resemble each other, we consider that the test piece has the thickness coating for this calculation.

We will re-design the thickness of each coated layers with the optical constant estimated by the measurements. We evaporate a multi-layer coated mirror for the broadband EUV range, and evaluate its reflectivity to put it to practical use.

Reference

1) I. Yoshikawa et al., *J. Geophys. Res.*, *102*, 19,897, 1997.

2) M. Nakamura et al., *Geophys. Res. Lett.*, *27*, 141, 2000.

3) I. Yoshikawa et al., *J. Geophys. Res.*, *106*, 26,057, 2001.

4) I. Yoshikawa et al., *Geophys. Res. Lett.*, *27*, 3,567, 2000a.

5) M. Nakamura et al., *UVSOR Activity Report*, 152, 1998.

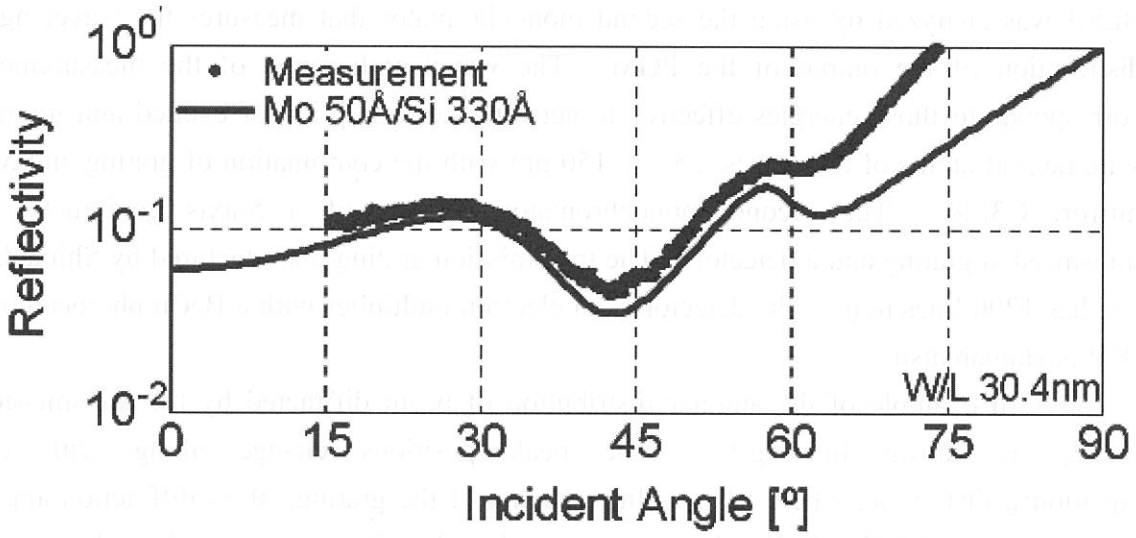

Figure. Reflectivity of the test Mo/Si multi-layer coated mirror. The points represent the measured value, and the black curve shows the calculation of the Mo 5nm/Si 33nm multi-layer reflectivity.

(BL5B)

Evaluation of higher order light of the PGM at BL5B

Makoto Sakurai, Takashi Adachi[1], Takato Hirayama[2], and Ichiro Arakawa[1]

Department of Physics, Kobe University, Kobe 657-8501

[1]Department of Physics, Gakushuin University, Toshima, Tokyo 171-8588

[2]Department of Physics, Rikkyo University, Toshima, Tokyo 171-8501

We have reported the results of measurements of absolute photo-desorption yields from the surface of solid Ne[1], Ar [2, 3] and Kr [4] by the irradiation of synchrotron radiation at excitonic excitation regime. Since the desorption yield depends on the energy of incident photon, the efficiency changes with the contribution of higher order light. Then, the higher order distribution of the output light of the monochromator (PGM) of BL5B was analyzed by using the second monochromator that measures the wavelength distribution of the output of the PGM. The wavelength range of the measurement corresponds to those energies effective to activate the desorption of excited and ground state neutral atoms of rare gases; 25 ～ 150 nm with the combination of grating and M2 mirror: G3M4. The second monochromator consists of a 5-axis goniometer, a transmission grating and a detector. The transmission grating manufactured by Shimadzu Co. has 1200 lines/mm. The detector is an electron multiplier with a BeCu photocathode (R595, Hamamatsu).

An example of the angular distribution of beam diffracted by the transmission grating is shown in Fig.1. The peak positions change along with the equation: $d \sin\theta = n\lambda$, where d is a line spacing of the grating, θ is diffraction angle, n is an order of diffraction, and λ is the wavelength. Broken curves show the change of the position of the first order diffraction peaks of the original wavelength, and dashed curves show those of the first order diffraction peaks of the second order light (i.e. with half of the original wavelength). Higher order contribution obviously increases with the wavelength.

Since the diffraction angles of the first order diffraction ($n=1$) of original wavelength (λ) and the second order diffraction ($n=2$) of the second order light ($\lambda/2$) coincide, theoretical diffraction efficiency of a transmission grating is used to determine the second order contribution. The relative photon number for each order light is calculated from the measured intensity taking into account the quantum efficiency of the detector, and is converted to the absolute photon number using the current of a beam

intensity monitor (a gold plate) as shown in Fig.2. Since the efficiency becomes higher when incident photon energy increases, the intensities of higher order in Fig.1 are too emphasized. The higher order lights are negligible for shorter wavelength region, however, they become comparable with the first order at wavelengths longer than 70 nm. These data are utilized to obtain the absolute desorption yield of rare gases.

References

[1] I. Arakawa, T. Adachi, T. Hirayama and M. Sakurai, Surf. Sci. **45**1, 136 (2000).

[2] T. Adachi, T. Hirayama, I. Arakawa and M. Sakurai, UVSOR Act. Rep. 1999, UVSOR-**2**7, 178 (2000).

[3] T. Adachi, T. Hirayama, I. Arakawa and M. Sakurai, UVSOR Act. Rep. 2000, UVSOR-**2**8, 208 (2001).

[4] T. Adachi, T. Hirayama, I. Arakawa and M. Sakurai, in preparation.

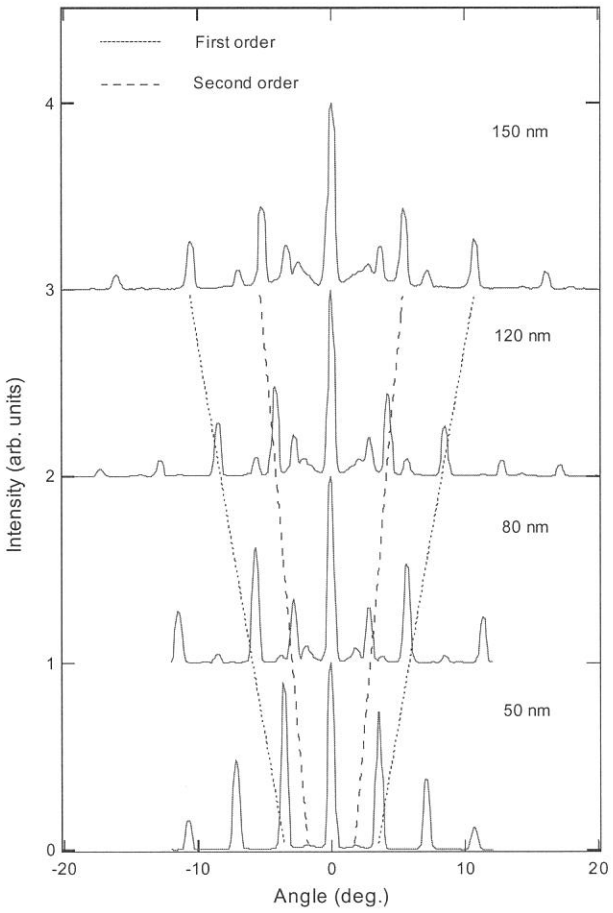

Fig.1 Angular distributions of the diffracted beams for various incident photon wavelengths.

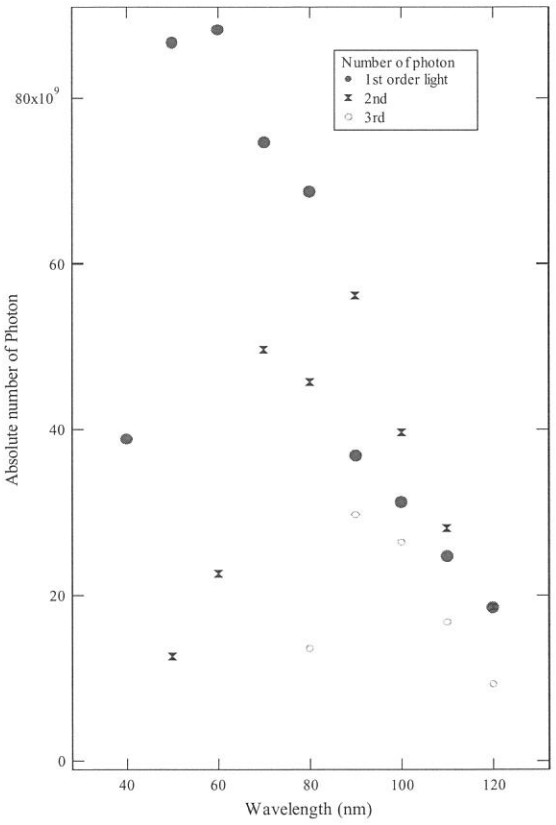

Fig.2 Photon number for each order light at various wavelengths.